

1 **Chemical ozone loss and chlorine activation in the Antarctic winters** 2 **2013–2020**

3
4 Raina Roy^{1,2*}, Pankaj Kumar¹, Jayanarayanan Kuttippurath^{1*}, Franck. Lefevre³

5
6 ¹*CORAL, Indian Institute of Technology Kharagpur, Kharagpur–721302, India.*

7 ²*Department of Physical Oceanography, Cochin University of Science and Technology, Kochi, India.*

8 ³*LATMOS/IPSL, Sorbonne Université, UVSQ, CNRS, Paris, France*

9
10 *Correspondence to:* R. Roy and J. Kuttippurath (rainaroy2105@gmail.com; jayan@coral.iitkgp.ac.in)

11 12 13 **Abstract**

14 The annual formation of an ozone hole in the austral spring has regional and global climate implications. Antarctic
15 ozone hole has already changed the precipitation, temperature and atmospheric circulation patterns, and thus, the
16 surface climate of many regions in the Southern Hemisphere (SH). Therefore, the study of ozone loss variability is
17 important to assess its consequential effects on the climate and public health. Our study uses satellite observations
18 from the Microwave Limb Sounder on Aura and the passive tracer method to quantify the ozone loss for the past
19 eight years (2013–2020) in the Antarctic. We observe the highest ozone loss (about 3.5 ppmv) in 2020, owing to
20 the high chlorine activation (about 2.2 ppbv), steady polar vortex, and huge expanses of polar stratospheric clouds
21 (PSCs) (12.6 million km²) in the winter. The spring of 2019 also showed a high ozone loss, although the year had
22 a rare minor warming in mid-September. The chlorine activation in 2015 (1.9 ppbv) was the weakest, and the wave
23 forcing from the lower latitudes was very high in 2017 (up to -60 Kms⁻¹). The analysis shows significant interannual
24 variability in the Antarctic ozone as compared to the immediate previous decade (2000–2010). The study helps to
25 understand the role of dynamics and chemistry in the interannual variability of ozone depletion over the years.

26 **Keywords:** Antarctic; Ozone loss estimates; Polar Vortex; Climate Change; Model simulations

27 **Short title:** Antarctic ozone loss in 2013–2020

32 **Introduction**

33

34 An important event in the Antarctic stratosphere during the austral spring that has caught global attention ever since
35 its discovery in the 1980s is the Antarctic ozone hole (Farman et al., 1985). The chlorine free radicals released from
36 the chlorofluorocarbons (CFCs) and other ozone-depleting substances (ODSs) activate the catalytic cycles that lead
37 to severe ozone loss (e.g., Stolarski and Cicerone, 1974; Rowland et al., 1976). The extreme cold conditions that
38 prevail in the poles facilitate the formation of Polar Stratospheric Clouds (PSCs), which serve as the activation
39 surface for the ODSs. Apart from these, the relatively stable Antarctic polar vortex also contributes significantly to
40 the annual formation of ozone holes (Solomon et al., 2014). Since the discovery of ODSs in the 1970s from
41 anthropogenic activities, ozone loss has continued to rise and reached its worst phase in the late 1980s and early
42 1990s (e.g., WMO, 2014). The increase in ODSs was curtailed after the enactment of the Montreal Protocol in
43 1987. Ratifying the environmental treaty led to a stabilisation of ozone loss from the late 1990s to the early 2000s
44 in the Antarctic. Despite this, there was no significant increase in total column ozone (TCO) during those times
45 (e.g., Weatherhead et al., 2000; WMO, 2007; Angell et al., 2009). Beyond 2000, significant recovery trends in the
46 lower stratospheric ozone were presented with evidence from both ground and satellite observations (e.g., Yang et
47 al., 2008; Salby et al., 2011; Solomon et al., 2016; Chipperfield et al., 2017; Kuttippurath and Nair, 2017; de Laat
48 et al., 2017; Pazmiño et al., 2018; Wespes et al., 2019; Johnson et al., 2023). A reduction in the saturation of ozone
49 loss over the period 2001–2017 is also observed in the Antarctic, confirming the positive ozone trends in the region
50 (Kuttippurath et al., 2018). There are also studies showing the changes in surface climate of Southern Hemisphere
51 (SH) due to ozone hole, by altering its temperature, winds, general circulation and precipitation. Therefore,
52 understanding of the Antarctic ozone variability is important for assessing the future changes in the climate of SH
53 (e.g., Gillett and Thompson, 2003; Polvani et al., 2011). For instance, the modelling studies of Kang et al. (2013)
54 and Brönnimann et al. (2017) show increased extreme precipitation in the austral summer in the southern high and
55 subtropical latitudes, and enhanced precipitation in the southern flank of South Pacific Convergence Zone,
56 respectively, due to the Antarctic ozone hole.

57 Here, we present the long-term analysis of ozone loss for the period 2013–2020 considering the chemical and
58 dynamical characteristics of the winters. Although a few of the years have been studied individually, the long-term
59 analysis helps in better understanding the evolution of the winters (e.g., WMO, 2015; Krummel et al., 2016;
60 Wargan et al., 2020; Manney et al., 2020; Klekociuk et al., 2021). The dynamics of these winters are studied using
61 different meteorological parameters. The study offers a high-resolution analysis of the interannual variability of

62 ozone at various altitudes using the data obtained from the Aura Microwave Limb Sounder (MLS) (Froidevaux et
63 al., 2008; Santee et al., 2008). The ozone loss is calculated using the passive tracer simulated by the REPROBUS
64 (Reactive Processes Ruling the Ozone Budget in the Stratosphere) chemical transport model (CTM) (Lefèvre et al.,
65 1994). Therefore, we use a single dataset and the same method to estimate ozone loss for all eight years to assess
66 the interannual variability, which would make the comparisons among the winters meaningful, coherent and robust.

67 **Data and Methods**

68 We have analysed the meteorology of the winters 2013–2020 using the Modern-Era Retrospective Analysis for
69 Research and Applications (MERRA-2) data (Gelaro et al., 2017) as these data include the information regarding
70 all weather parameters such as temperature and winds, planetary waves, heat flux and polar stratospheric clouds
71 (PSCs). MERRA 2 data are available for 42 pressure levels at a spatial resolution of $0.5^\circ \times 0.625^\circ$. The nature of
72 austral springs is studied by the polar cap temperature zonally averaged between 60° and 90° S at 100 hPa, the
73 minimum polar cap temperature at 10 hPa, the area of PSCs at 460 K, and the mean heat flux averaged over the
74 latitude band 45° – 75° S. The PSC area is estimated using the amount of water vapour of 5 ppm and nitric acid of
75 4.97 ppt at 460 K. Further details are provided on
76 https://ozonewatch.gsfc.nasa.gov/meteorology/temp_2022_MERRA2_SH.html). Besides, the MERRA 2 dataset is
77 also employed to analyse the vertical evolution of temperature averaged over 60° – 90° S.

78 The ozone loss is estimated using the passive tracer method (e.g. Kuttippurath et al., 2015). The tracer is simulated
79 by the REPROBUS CTM, which is identical to ozone, but without interactive chemistry. It is a three-dimensional
80 model driven by the European Centre for Medium-Range Weather Forecasts (ECMWF) operational analyses. The
81 analysis is performed for the altitude range of 1000–0.01 hPa (137 levels). In the model, the advection is performed
82 by the winds on the hybrid sigma-pressure coordinates, and the trace gases are advected by a semi-lagrangian
83 technique (Williamson and Rasch, 1989). In our study, the passive tracer is initialised on 1st of June each year and
84 continued until the end of November. The loss is then computed by subtracting the measured ozone from the
85 modelled passive ozone, which is also called inferred ozone loss. Note that the model simulations are used only for
86 the passive ozone in this study. Since the tracer initialisation was made on 1st of April in 2020, there was a
87 consequential offset in its values with respect to other years on 1st of June. This offset is corrected for the ozone
88 loss computation for that year. The loss in each day is estimated inside the polar vortex as it is more prevalent there,
89 and the vortex edge is calculated using the equivalent latitude (Nash et al., 1996; Müller et al., 2005). The
90 measurements of ozone and chlorine monoxide (ClO) are taken from the MLS version 4.2. These ozone data have

91 a vertical resolution of 2–3 km, a vertical range of 261–0.02 hPa and an accuracy of 0.1–0.4 ppmv. The ClO
92 measurements are performed at 640 GHz, and these data have a vertical resolution of 3–3.5 km at 147–1 hPa with
93 an accuracy of about 0.2–0.4 ppbv. These ClO measurements have a latitude-dependent bias of around 0.2–0.4
94 ppbv, depending on the altitude (Livesey et al., 2013).

95 **Results and Discussion**

96 **Meteorology of the winters**

97
98 Fig. 1 shows the meteorology of the winters as illustrated with the polar cap temperature (60–90° S) at 100 hPa,
99 the minimum temperature averaged over 50°–90° S at 100 hPa, PSC area at 460 K and the heat flux averaged
100 between 45° and 75° S at 100 hPa. The top panel shows the mean temperature (60°–90° S) at 100 hPa, and the
101 coloured lines represent individual years. Temperature decreases from the beginning of winter (June) onwards and
102 reaches its lowest in August. The lowest temperature for most years is observed in August, but it continued to
103 September in 2015 and 2020. Temperature is in the order of 195–208 K during this period in most years (Fig. 1).
104 In the years 2013, 2014, 2015 and 2020, the temperature shows below 195 K (the PSC formation threshold).
105 However, the temperature shows a sudden rise from late August (202 K) to mid-September (218 K) in 2019,
106 indicative of the occurrence of a Sudden Stratospheric Warming (SSW). This event has been reported in some of
107 the previous studies and has been described as a minor Warming (mW) (e.g., Shen et al., 2020a,b; Yamazaki et al.,
108 2020; Roy et al., 2022). Temperature in August 2017 is also higher than that in previous years but lower than in
109 2019. There is a rise in temperature at the beginning of the austral spring. However, temperatures persist below
110 195 K during early September 2015. The lowest temperatures during the winter–spring period are found in 2015
111 and 2020, as depicted in Fig. 1.

112 Fig. 1 (second panel from top) shows the minimum polar cap temperature for each winter, and is lower than the
113 PSC formation threshold (195 K). This continues in the early spring for all years except in 2019, and the minimum
114 value rises soon after and is higher than 195 K in the late spring. The minimum temperature reaches this threshold
115 for most days and thus, the ideal conditions for the formation of PSCs are found in all winters. Therefore, the PSC
116 area has grown since the beginning of winter and is highest in August (up to 28 million km²). Corresponding to the
117 periods of longest duration of minimum temperature, PSCs persist until early November in 2015, 2018 and 2020,
118 but are relatively short-lived in 2017 and 2019. As the mean temperature peaks in early to mid-September 2019,
119 the PSC area drops and diminishes by late September. However, the PSCs dissipated by mid-October in 2017.

120 A major factor affecting the strength of polar vortex is tropospheric forcing. Strength of this forcing is very weak
121 in the Antarctic, except for a few winters. According to Zuev et al. (2019), the strengthening of Antarctic polar
122 vortex in winter and spring is due to the seasonal temperature variations in the subtropical lower stratosphere. Fig.
123 1 (bottom) shows the tropospheric forcing estimated for all years. The heat flux averaged between the adjacent
124 mid-latitudes and higher latitudes is directed southward, particularly in the late winter and early spring. The years
125 2019 and 2017 are characterised by very strong wave forcing, as shown by the high flux values (from -40 to -50
126 Kms^{-1}). Klekociuk et al. (2020) reported that the easterly phase of QBO favoured the enhanced wave activity in
127 2017; a reason for the relatively higher temperature in that winter. Milinevsky et al. (2019) and Evtushevsky et al.
128 (2020) also found similar results for both winters. The zonal average of heat flux stays between -30 and 10 Kms^{-1}
129 for most winters, and the flux increases as the spring approaches. However, these forcings are weak in the years
130 2015 and 2020.

131 **Temporal evolution of temperature with altitude**

132 Fig. 2 shows the temporal evolution of zonal mean (60° – 90° S) temperature profiles in the Antarctic for the years
133 2013–2020. The coloured contours show the temperature across the seasons and white contour lines represent 188,
134 195 and 210 K. Here, the zonal winds (westerlies) are overlaid with black contours, and the easterlies are in red. In
135 general, temperature increases towards the end of spring in the stratosphere, but it started to rise in the lower
136 stratosphere much earlier during the spring of 2019 and 2017. Temperature contours of 250–265 K extend to
137 slightly below 10 hPa and there is a small reduction in the speed of westerlies during the period. Temperatures
138 below 195 K are found in the lower stratosphere (100–70 hPa) until mid-October in 2015 and 2020. Similarly, the
139 area covered by < 195 K was also moderately large in 2013, 2014, 2016 and 2018. However, this is lowest in 2019
140 and relatively very small in 2017. The appearance of easterlies below 10 hPa is late (end of November) and thus,
141 the vortex lasted longer in 2015 and 2020, whereas as early as late October in 2017 and 2019. We also made an
142 assessment inside the vortex, to examine the consistency of our analysis with and without the vortex criterion (see
143 Figure S1). The key features are same in both analyses, such as the very low temperatures in the lower stratosphere,
144 strong westerlies and late appearance of easterlies in the middle stratosphere in 2015 and 2020, the early appearance
145 of easterlies and the minor warming in 2019, and the large and extended period of PSC threshold temperature (195
146 K) in 2018. Since the meteorology is different inside the vortex, small differences in the temperature (e.g., PSC
147 threshold area) and wind (middle stratospheric westerlies in 2015 and 2020) values are also found between the two.

148

150 Fig. 3 shows the temporal evolution of ozone (in ppmv) inside the vortex deduced from the MLS data for the period
151 2013–2020. The ozone is lost in the lower altitudes as time progresses in spring, as illustrated in Fig. 3. It is observed
152 from previous studies that the ozone loss is maximum in the lower stratosphere in all years (Solomon et al., 1999).
153 Contrary to this, ozone increases in the upper stratosphere as the winter progresses towards spring. Ozone in the
154 lower stratosphere (400–600 K) is around 0.1–3 ppmv in 2013, 2014, 2015, 2016, 2018 and 2020. Unlike in the
155 cold winters, ozone is slightly higher (by 0.5–1.5 ppmv) in the lowermost stratosphere in 2019. Similarly, in 2017,
156 ozone in the lower stratosphere (400–450 K) is higher than that in the previous cold years, owing to the higher
157 temperature there. The lowest ozone for the altitude range of 400–475 K is observed in 2015, 2018 and 2020, in
158 which the 0.5 ppmv contour extends to 475–500 K.

159 Figure 4 presents the temporal evolution of ClO (right) and ozone loss (left) at different altitudes during the period
160 of study. Since there are unreasonably high tracer values in June due to initialisation problem, the ozone loss is not
161 calculated up to 10 June 2018 and 20 July 2019. In general, ozone loss is highest at 400–550 K (lower stratosphere)
162 during September and October in all years. The loss is smaller than 1.4 ppmv in the upper stratosphere, mostly
163 driven by the NO_x-based chemistry (e.g., Kuttippurath et al., 2015). The loss in 2014 and 2015 is almost similar,
164 about 2.6–3.0 ppmv at the peak ozone loss altitude (450–550 K) during September and October. The loss in 2013
165 reaches up to 3.0 ppmv by mid-October and is higher than in 2014, 2015, 2017 and 2018 (e.g., Vargin et al., 2020).
166 The ozone loss reported by Strahan et al. (2018) for 2015 is similar to the very cold winters in Antarctica and is
167 slightly higher than our estimate for that winter. The ozone loss with altitude is larger in 2015 than other winters
168 (see Fig. 4). The preconditioning for ozone loss in 2013 and 2014 was ensured by high chlorine activation at the
169 same altitude range (Kuttippurath et al., 2015). Among these three years (2013–2015), before the period of highest
170 ozone loss, chlorine activation reaches its peak in August and September. ClO amounts up to 2.2 ppbv in 2013 and
171 2014, and 2.0 ppbv in 2015 during this period. This high chlorine activation lasted for almost a month at the peak
172 ozone loss altitudes (450–550 K) in 2013, but for a relatively shorter period in 2014 and 2015. Similar values for
173 ozone loss and ClO (1.8–2.2 ppbv) are also estimated for 2017 and 2018, and the highest ClO stayed intact for 15–
174 20 days before attaining the maximum ozone loss.

175

176 The ozone loss in 2016 is about 3–3.2 ppmv in September and 3.4 ppmv in October. Note that the ozone hole, PSC
177 occurrence and chlorine activation (more than a month, up to 2.2 ppbv) lasted longer in this year. An extensive

178 ozone hole from late August to mid-November is found in 2019. However, ozone increased after the minor
179 warming, and thus the ozone hole size (Fig. 3) and ozone loss reduced significantly thereafter (Fig. 4). The chlorine
180 activation was very strong and continuous from August to September (above 2.2 ppbv) in this year. Despite the
181 minor warming, the ozone loss in 2019 (3.0–3.4 ppmv) is similar to that in 2016. The nature of spring 2019 was
182 similar to the previous warm Antarctic years of 1988 and 2002, as the vortex was short-lived and highly variable
183 due to strong tropospheric forcing and SSW (Manney et al., 2020; Klekociuk et al., 2021). The peak ozone loss in
184 2019 is about 3.4 ppmv, which is higher than that in other winters, except 2020 (Wargan et al., 2020; Roy et al.,
185 2022). The chlorine activation remained at its peak value (2.0–2.2 ppbv) for several days in August before reaching
186 the peak ozone loss in 2019, and the spatial distribution (450–550 K) of these high ClO values is the largest
187 compared to all other years. The 2020 ozone loss is very high (up to 3.6 ppmv) and exceeds the maximum ozone
188 loss of other winters. The chlorine activation rose in the early spring (September) (2.0–2.2 ppbv) and is similar to
189 that in 2016. The high values of ozone loss may have resulted from the increased aerosol loading from the
190 Australian bushfires in 2020 (e.g., Stone et al., 2021). A recent study by Ansmann et al. (2022) shows that about
191 10–20% of the ozone loss in 2020 was driven by the wildfire smoke that caused the growth of PSC particles.

192

193 **Interannual variability of ozone loss**

194

195 The interannual variability of ozone loss, PSC and chlorine activation is shown in Fig. 5. Here, the ozone loss is
196 computed by taking the average of ozone loss from day 270 to 300 (the peak loss period) in the altitude range 450–
197 550 K (the peak loss altitudes, see Fig. 4). Similarly, the chlorine activation is indicated as the average of ClO over
198 the same altitude range, but for the days between 210 and 270 (peak chlorine activation period). The weighted
199 mean of PSC area is shown with black solid line for the years 2013–2020. Note that the peak ozone loss duration
200 and altitude range are different in different winters (e.g. 2018 and 2020). The smallest ozone loss is estimated for
201 the years 2015 and 2017 because of relatively weak chlorine activation in those winters. The mean ozone loss is
202 about 2.4 ppmv and ClO is about 1.75–1.95 ppbv in both years. However, the PSC area in 2015 (11.9 million km²)
203 was higher than most of other cold winters. The larger PSC area is mostly because of the lower temperature
204 conditions that lasted longer in the winter. Tully et al. (2019) identified 2015 as one of the most severe and extreme
205 winters, as also observed in our study. The PSC area in 2017 (10.2 million km²) is smaller and therefore, ozone
206 loss is lower as compared to that in 2015, which is consistent with the results of Braathen (2018).

207

208 The highest ozone loss is estimated in 2020 (3.1 ppmv) in the spring, which is followed by 2016 (3.0 ppmv). The
209 chlorine activation for both years is also higher than that of a few other cold winters, as shown by the ClO values
210 of about 2.1–2.2 ppbv. The highest ozone loss in 2020 is favoured by the very large PSC area (12.6 million km²).
211 The 2018 spring was also unique in comparison to the other years as a consequence of the high chlorine activation
212 (2.2 ppbv) and very large PSC area (12.0 million km²). The chlorine activation was very high in 2019 (2.1 ppbv),
213 but the relatively lower ozone loss during this particular period is a direct consequence of its unfavourable dynamic
214 condition (SSW). The PSC area is also lowest in 2019 (9.4 million km²) among the winters due to SSW. The ozone
215 loss (2.7–2.8 ppmv) and chlorine activation (2.1–2.2 ppbv) are similar in other winters.

216
217 Table 1 shows the partial column ozone loss estimated with the MLS data and REPROBUS passive ozone
218 simulations for two different altitude ranges. The partial column loss at 350–750 K yields similar values for most
219 winters, as the highest loss is estimated for 2015, 2016, 2018 and 2019 (around 163±16 DU), consistent with the
220 meteorology of the winters. However, the lowest column loss (128±12 DU) is estimated for the winter 2020, as the
221 vertical spread of ozone loss is limited beyond the peak ozone loss altitude range of 450–550 K in this winter (see
222 Fig. 4). Similarly, ozone loss in the moderately cold winters shows a loss of about 154±15 DU (2013 and 2014),
223 but very small loss in 2017 (134±13 DU). The column loss computed at 400–600 K, the highest ozone loss altitudes
224 in the Antarctic, has slightly lower values as expected. In general, there is an average difference of about 40 DU
225 (higher than the 400–600 K) ozone loss between these altitude ranges (e.g., Kuttippurath et al., 2015). The loss is
226 highest in 2019 (145±14 DU) at 400–600 K as in the case of 350–750 K, but smallest in 2015 (107±10 DU). This
227 suggests that there is higher ozone loss at altitudes above 600 K in the very cold winter of 2015 (see Fig. 4). On
228 the other hand, ozone loss and its difference between these two altitude ranges are very small for 2020 and 2017,
229 as discussed before.

230

231 **Conclusions**

232 We analyse the ozone loss for the past 8 years (2013–2020) in the Antarctic. The year 2019 had a warm winter
233 with a mW in mid-September. The winter of 2017 also shows similar characteristics, such as the sudden increase
234 in temperature during late August, higher minimum temperature (about 205 K) in August than in other years and
235 the sharp decrease in PSC area towards the end of September. The heat flux magnitude for the year (2017) is also
236 higher than that in other winters (up to -60 Kms⁻¹), suggesting that it was a disturbed warm winter. We find a
237 minimal ozone loss in 2017 and it stayed less than 2.8 ppmv (110±11 DU at 400–600 K) for most of October and

238 September. Chlorine activation was also below 1.8 ppbv during August and September in the year. Conversely, the
239 wave fluxes are lowest in 2015. The temperature and PSC area follow similar temporal evolution in 2013, 2014,
240 2015, 2016 and 2018. Winter 2020 exhibits unique meteorology with a long-lasting occurrence of vortex-wide
241 PSCs (12.6 million km²) and thus, shows the highest ozone loss (3.5 ppmv). On the other hand, the lowest ozone
242 loss (2.5 ppmv or 107±10 DU at 400–600 K) is estimated in 2015. Our study, thus, helps in understanding how the
243 chlorine activation and meteorology of the winters influence the variability of ozone. Dynamics and chemistry of
244 the winters play their respective roles in the ozone loss process. The winter of 2019 is an example of favourable
245 chemistry helping in large loss in ozone, though the dynamical conditions were unfavourable.

246 **Acknowledgements**

247 We thank the Chairman of CORAL and the Director of Indian Institute of Technology Kharagpur for facilitating
248 the study. We acknowledge free use of the MLS data, which are taken from <https://disc.gsfc.nasa.gov/>. The
249 meteorological data are acquired through <https://ozonewatch.gsfc.nasa.gov/>. The REPROBUS data are acquired
250 through IPSL, <http://cds-espri.ipsl.fr/>. We thank Cathy Boone for her help with the REPROBUS model runs,
251 analyses and data transfer, and IPSL for hosting the data.

253 **Data availability**

254 The data used in this study are publicly available. The MLS data are available from <https://disc.gsfc.nasa.gov/>. The
255 meteorological data are acquired through <https://ozonewatch.gsfc.nasa.gov/>. The REPROBUS data are acquired
256 through IPSL, <http://cds-espri.ipsl.fr/>. The analysed data/codes can also be provided on request.

258 **Competing Interests**

259 JK is an Editor of Atmospheric Chemistry and Physics. Otherwise, no competing interests.

261 **Author Contributions**

262 JK conceived the idea, and JK and RR wrote the original manuscript. The manuscript was subsequently revised
263 with inputs from PK and FL. The model runs and model results were analyzed by FL. The data analyses and figures
264 made by RR and PK. All authors participated in discussions and made suggestions, which were considered for the
265 final draft.

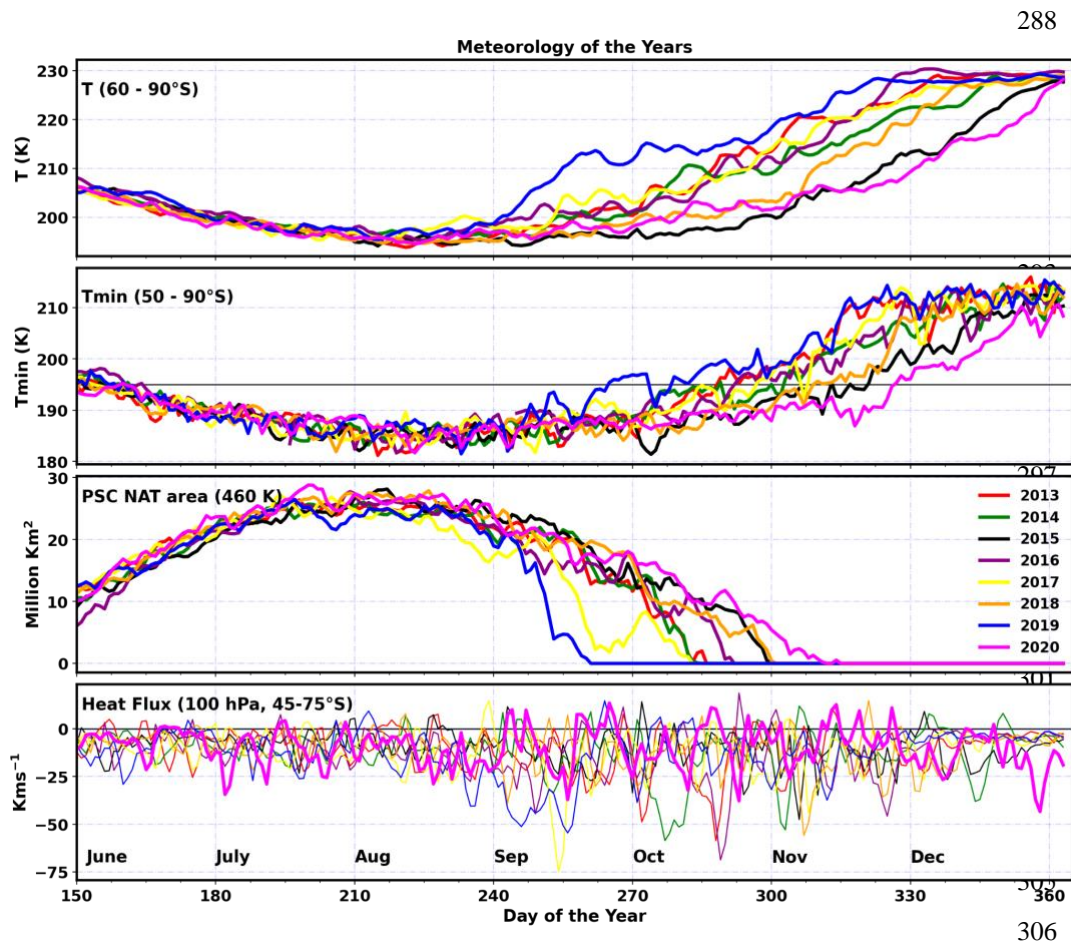
266

267 **Table 1:** The partial column ozone loss computed using the MLS ozone measurements and modelled tracer by
268 applying the passive method. The column loss is estimated for the peak ozone altitude ranges of 350–750 K and
269 400–600 K. The ozone column loss estimates have an uncertainty of about 10%.

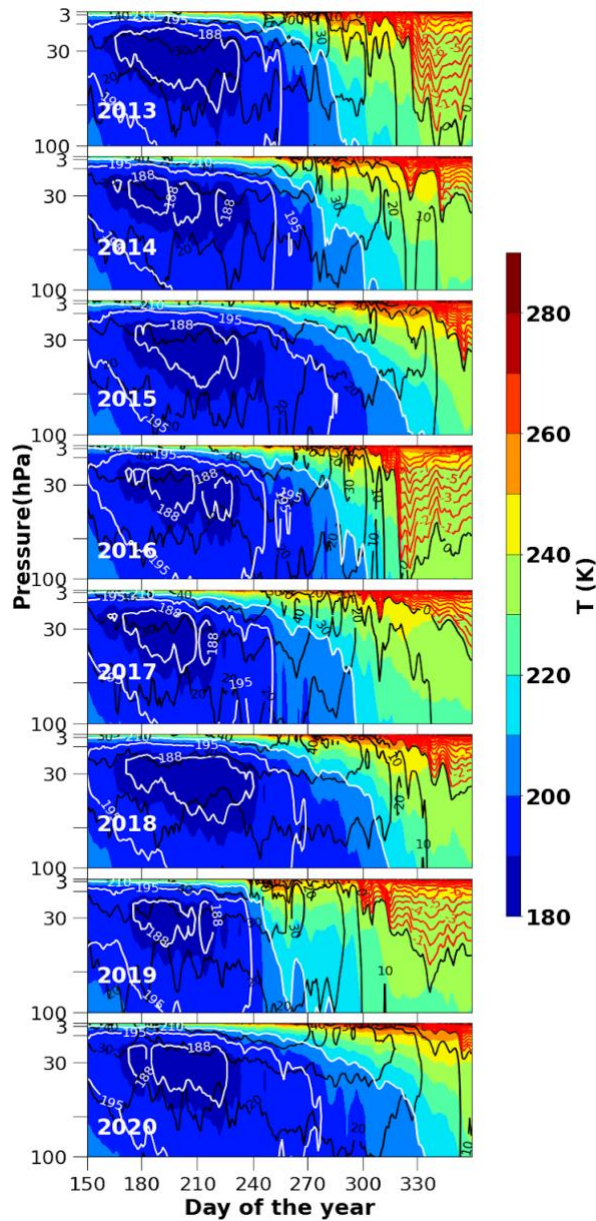
Year	Ozone column loss 350–750 K (DU)	Ozone column Loss 400–600 K (DU)
2013	153	122
2014	156	122
2015	169	107
2016	163	128
2017	134	110
2018	165	115
2019	169	145
2020	128	120

270
271
272
273
274
275
276
277
278
279
280
281
282
283

284
285
286
287



307 **Figure 1:** Meteorology of the years (2013–2020). Top panel shows the zonal average temperature (60° – 90° S) at
308 100 hPa. Second panel (from top) shows the minimum temperature at 100 hPa. The black horizontal line in the
309 panels shows 195 K (PSC formation threshold). Third panel (from top) shows the PSC area at 460 K and the bottom
310 panel shows the mean heat flux (45° – 75° S) at 100 hPa. The black horizontal line in the bottom panel shows zero
311 heat flux.
312



313

314 **Figure 2:** Seasonal march of the zonal mean temperature for the period 2003–2020 averaged over the latitudes

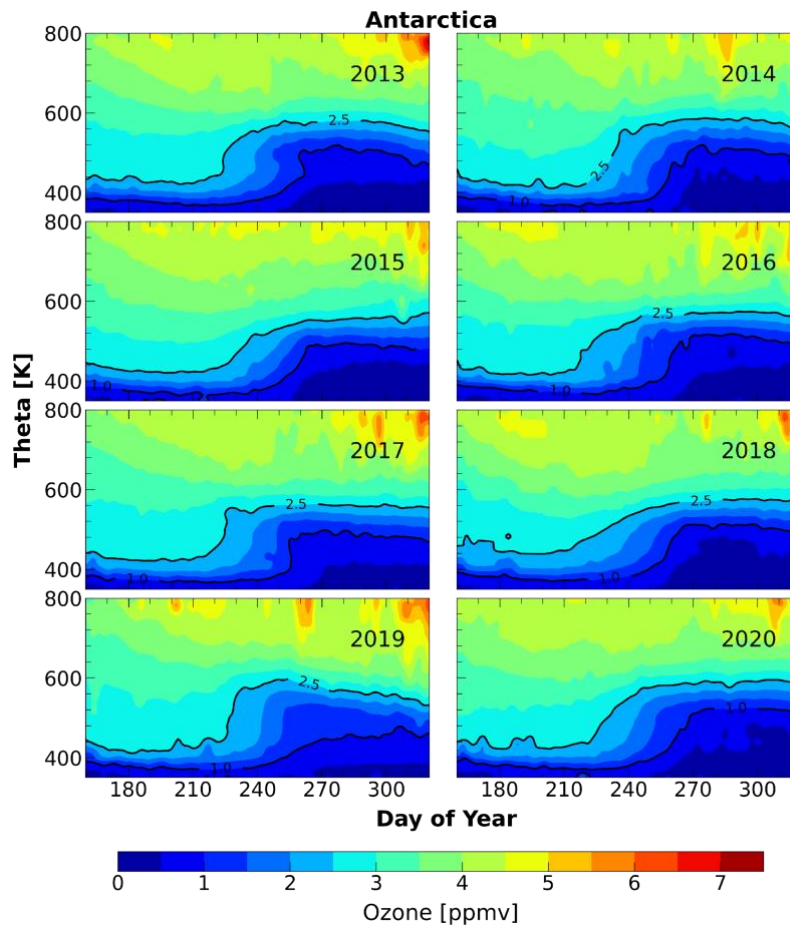
315 60° – 90° S. The contours show the temperature and white contours represent specific temperatures such as 188, 195

316 and 210 K. The zonal wind velocities are overlaid. The black contour lines show the westerlies and the red contour

317 lines show the easterlies.

318

319



320
321

322 **Figure 3:** Temporal evolution of the vertical profiles of ozone averaged inside the vortex for the winters 2013–
323 2020 in the Antarctic. The temporal evolution is analysed using the MLS ozone data at 350–800 K for the period
324 June–November. The black contours represent 1.0 and 2.5 ppm of ozone.

325

326

327

328

329

330

331

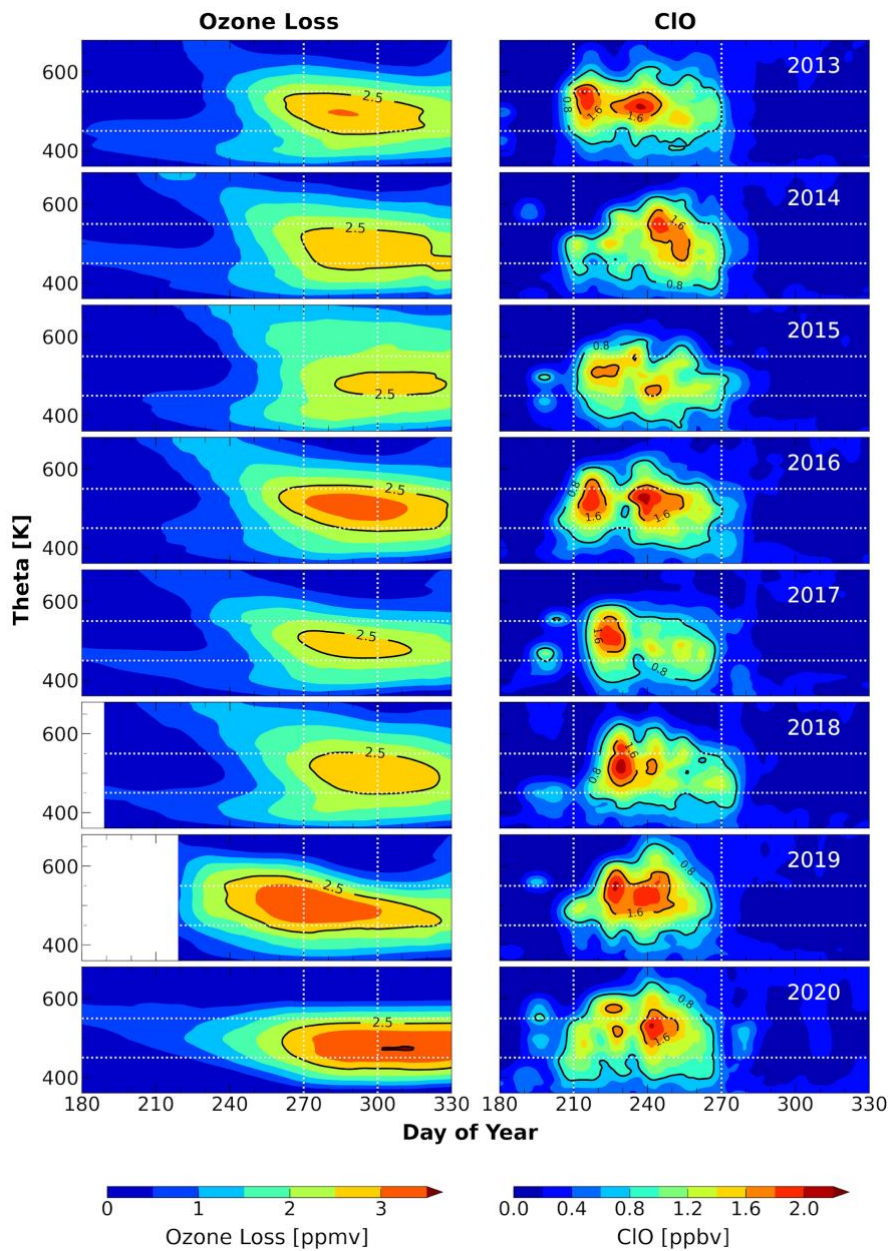
332

333

334

335

336

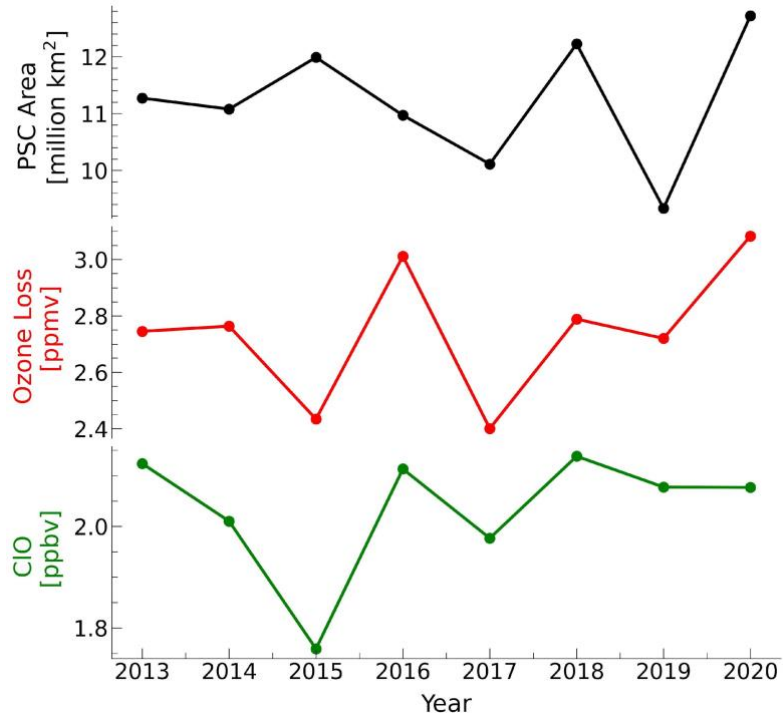


337
338
339
340
341
342
343

Figure 4: Temporal evolution of ozone loss estimated from MLS measurements using REPROBUS passive tracer (left). The MLS CIO measurements for the altitude range 350–700 K for the period 2013–2020 (right). The ozone loss estimates and CIO measurements are selected inside the polar vortex as per the Nash et al. (1996) criterion. Ozone loss is not computed up to 10th June in 2018 and 20th July in 2019 because of the unavailability of tracer values. The black contours represent 2.5 and 3.5 ppm of ozone loss (left panel) and 0.8 and 1.6 ppb of CIO (right panel).

344

345



346

347 **Figure 5:** The vortex-averaged ozone loss estimated from the MLS measurements using the passive method, peak
348 ClO measurements, and the weighted average of area of PSC for the period 2013–2020. The mean ozone loss is
349 estimated over the altitude range 450–550 K and between day 270 and 300 (maximum ozone loss days). The ClO
350 measurements are averaged over the altitude range 450–550 K and between day 210 and 270; representing the
351 strong chlorine activation period and altitudes.

352

353

354

355

356 **References**

- 357 Angell, J. K. and Free, M.: Ground-based observations of the slowdown in ozone decline and onset of ozone
358 increase, *J. Geophys. Res.*, 114, D07303, doi:10.1029/2008JD010860, 2009.
- 359 Ansmann, A., Ohneiser, K., Chudnovsky, A., Knopf, D. A., Eloranta, E. W., Villanueva, D., Seifert, P., Radenz,
360 M., Barja, B., Zamorano, F., Jimenez, C., Engelmann, R., Baars, H., Griesche, H., Hofer, J., Althausen, D., and
361 Wandinger, U.: Ozone depletion in the Arctic and Antarctic stratosphere induced by wildfire smoke, *Atmos.*
362 *Chem. Phys.*, 22, 11701–11726, doi:10.5194/acp-22-11701-2022, 2022.
- 363 Bandoro, J., Solomon, S., Donohoe, A., Thompson, D.W.J., and Santer, B.D.: Influences of the Antarctic ozone
364 hole on Southern Hemispheric summer climate change, *J. Climate*, 27(16), 6245–6264, doi: 10.1175/JCLI-D-13-
365 00698.1, 2014.
- 366 Braathen, G. O.: Observations of the Antarctic Ozone Hole from 2003 to 2017, p. 16503, 2018.
- 367 Brönnimann, S., Coper, J.M.*, Rozanov, E., Fischer, A.M.*, Morgenstern, O., Zeng, G., Akiyoshi, H., &
368 Yamashita, Y.: Tropical circulation and precipitation response to ozone depletion and recovery. *Environmental*
369 *Research Letters*, 12 (6), <https://doi.org/10.1088/1748-9326/aa7416>, 2017.
- 370 Butler, A., Daniel, J. S., Portmann, R. W., Ravishankara, A., Young, P. J., Fahey, D. W., and Rosenlof, K. H.:
371 Diverse policy implications for future ozone and surface UV in a changing climate, *Environ. Res. Lett.*, 11,
372 064017, doi:10.1088/1748-9326/11/6/064017, 2016.
- 373 Chipperfield, M. P., Bekki, S., Dhomse, S., Harris, N. R., Hassler, B., Hossaini, R., Steinbrecht, W.,
374 Thiéblemont, R., and Weber, M.: Detecting recovery of the stratospheric ozone layer, *Nature*, 549, 211,
375 doi:10.1038/nature23681, 2017.
- 376 de Laat, A. T. J., van Weele, M., and van der A, R. J.: Onset of stratospheric ozone recovery in the Antarctic
377 ozone hole in assimilated daily total ozone columns, *J. Geophys. Res.-Atmos.*, 122, 11880–11899,
378 doi:10.1002/2016JD025723, 2017.
- 379 Evtushevsky, O. M., Klekociuk, A. R., Kravchenko, V. O., Milinevsky, G. P., and Grytsai, A. V.: The influence
380 of large amplitude planetary waves on the Antarctic ozone hole of austral spring 2017, *J. South. Hemisph. Earth*
381 *Syst. Sci.*, 69, 57–64, doi:10.1071/ES19022, 2019.
- 382 Farman, J. C., Gardiner, B. G., and Shanklin, J. D.: Large losses of total ozone in Antarctica reveal seasonal
383 ClOx/NOx interaction, *Nature*, 315, 207-210, 1985.

384 Froidevaux, L., Jiang, Y. B., Lambert, A., Livesey, N. J., Read, W. G., Waters, J. W., Browell, E. V., Hair, J. W.,
385 Avery, M. A., McGee, T. J., Twigg, L. W., Summicht, G. K., Jucks, K. W., Margitan, J. J., Sen, B., Stachnik, R.
386 A., Toon, G. C., Bernath, P. F., Boone, C. D., Walker, K. A., Filipiak, M. J., Harwood, R. S., Fuller, R. A.,
387 Manney, G. L., Schwartz, M. J., Daffer, W. H., Drouin, B. J., Cofield, R. E., Cuddy, D. T., Jarnot, R. F., Knosp,
388 B. W., Perun, V. S., Snyder, W. V., Stek, P. C., Thurstans, R. P., and Wagner, P. A.: Validation of Aura
389 Microwave Limb Sounder stratospheric ozone measurements, *J. Geophys. Res.*, 113, 15–20,
390 <https://doi.org/10.1029/2007JD008771>, 2008.

391 Gelaro, R., McCarty, W., Suárez, M. J., Todling, R., Molod, A., Takacs, L., Randles, C. A., Darmenov, A.,
392 Bosilovich, M. G., Reichle, R., Wargan, K., Coy, L., Cullather, R., Draper, C., Akella, S., Buchard, V., Conaty,
393 A., da Silva, A. M., Gu, W., Kim, G.-K., Koster, R., Lucchesi, R., Merkova, D., Nielsen, J. E., Partyka, G.,
394 Pawson, S., Putman, W., Rienecker, M., Schubert, S. D., Sienkiewicz, M., and Zhao, B.: The Modern-Era
395 Retrospective Analysis for Research and Applications, Version 2 (MERRA-2), *J. Climate*, 30, 5419–5454,
396 <https://doi.org/10.1175/JCLI-D-16-0758.1>, 2017.

397 Gillett, N. P., Thompson, D. W.: Simulation of recent southern hemisphere climate change, *Science* (New York,
398 N.Y.), 302(5643), 273–275, <https://doi.org/10.1126/science.1087440>, 2003.

399 Johnson, B. J., Cullis, P., Booth, J., Petropavlovskikh, I., McConville, G., Hassler, B., Morris, G. A., Sterling, C.,
400 and Oltmans, S.: South Pole Station ozonesondes: variability and trends in the springtime Antarctic ozone hole
401 1986–2021, *Atmos. Chem. Phys.*, 23, 3133–3146, <https://doi.org/10.5194/acp-23-3133-2023>, 2023.

402 Kang, S. M., Polvani, L. M., Fyfe, J. C., Son, S.-W., Sigmond, M., Correa, G. J. P.: Modeling evidence that
403 ozone depletion has impacted extreme precipitation in the austral summer, *Geophys. Res. Lett.*, 40, 4054–4059,
404 [doi:10.1002/grl.50769](https://doi.org/10.1002/grl.50769), 2013.

405 Klekociuk, A., Tully, M. B., Krummel, P. B., Evtushevsky, O., Kravchenko, V., Henderson, S. I., et al.: The
406 Antarctic ozone hole during 2017, University Of Tasmania, Journal contribution,
407 <https://hdl.handle.net/102.100.100/558640>, 2020.

408 Klekociuk, A. R., Tully, M. B., Krummel, P. B., Henderson, S. I., Smale, D., Querel, R., Nichol, S., Alexander,
409 S. P., Fraser, P. J., and Nedoluha, G.: The Antarctic ozone hole during 2018 and 2019, *J. South. Hemisphere*
410 *Earth Syst. Sci.*, 71, 66–91, [doi:10.1071/ES20010](https://doi.org/10.1071/ES20010), 2021.

411 Krummel, P. B., Fraser, P. J., and Derek, N.: The 2015 Antarctic ozone hole and ozone science summary: final
412 report, CSIRO: Australia, iv, 27 pp, 2016.

413 Kuttippurath, J., Kumar, P., Nair, P. J., and Pandey, P. C.: Emergence of ozone recovery evidenced by reduction
414 in the occurrence of Antarctic ozone loss saturation, *Npj Climate and Atmospheric Science*, 1(1),
415 [doi:10.1038/s41612-018-0052-6](https://doi.org/10.1038/s41612-018-0052-6), 2018.

416 Kuttippurath, J., and Nair, P. J.: The signs of Antarctic ozone hole recovery, *Sci. Rep.*, 7, 585,
417 doi:10.1038/s41598-017-00722-7, 2017.

418 Kuttippurath, J., Godin-Beekmann, S., Lefèvre, F., Santee, M. L., Froidevaux, L., and Hauchecorne, A.:
419 Variability in Antarctic ozone loss in the last decade (2004–2013): high-resolution simulations compared to Aura
420 MLS observations, *Atmos. Chem. Phys.*, 15, 10385–10397, <https://doi.org/10.5194/acp-15-10385-2015>, 2015.

421 Langematz, U., and Kunze, M.: An update on dynamical changes in the Arctic and Antarctic stratospheric polar
422 vortices, *Clim Dyn*, 27, 647–660, <https://doi.org/10.1007/s00382-006-0156-2>, 2006.

423 Lefèvre, F., Brasseur, G. P., Folkins, I., Smith, A. K., and Simon, P.: Chemistry of the 1991/1992 stratospheric
424 winter: three-dimensional model simulations, *J. Geophys. Res.*, 99, 8183–8195, 1994.

425 Livesey, N. J., Read, W. G., Froidevaux, L., Lambert, A., Manney, G. L., Pumphrey, H. C., Santee, M. L.,
426 Schwartz, M. J., Wang, S., Cofeld, R. E., Cuddy, D. T., Fuller, R. A., Jarnot, R. F., Jiang, J. H., Knosp, B. W.,
427 Stek, P. C., Wagner, P. A., and Wu, D. L.: Earth Observing System (EOS) Aura Microwave Limb Sounder
428 (MLS) Version 3.3 and 3.4 Level 2 data quality and description document, JPL D-33509, Propulsion Laboratory,
429 California Institute of Technology, Pasadena, California, USA, 1–164, 2013.

430 Manney, G. L., Livesey, N. J., Santee, M. L., Froidevaux, L., Lambert, A., Lawrence, Z. D., et al.: Record-low
431 Arctic stratospheric ozone in 2020: MLS observations of chemical processes and comparisons with previous
432 extreme winters, *Geophys. Res. Lett.*, 47, e2020GL089063, <https://doi.org/10.1029/2020GL089063>, 2020.

433 Milinevsky, G., Evtushevsky, O., Klekociuk, A., Wang, Y., Grytsai, A., Shulga, V., Ivaniha, O.: Early indications
434 of anomalous behaviour in the 2019 spring ozone hole over Antarctica, *Int. J. Remote Sens.*, 41, 7530–7540,
435 <https://doi.org/10.1080/2150704X.2020.1763497>, 2020.

436 Müller, R., Tilmes, S., Konopka, P., Groß, J.-U., Jost, H.-J.: Impact of mixing and chemical change on ozone-
437 tracer relations in the polar vortex, *Atmos. Chem. Phys.*, 5, 3139–3151, <https://doi.org/10.5194/acp-5-3139-2005>,
438 2005.

439 Nash, E. R., Newman, P. A., Rosenfield, J. E., Schoeberl, M. R.: An objective determination of the polar vortex
440 using Ertel’s potential vorticity, *J. Geophys. Res.*, 101, 9471–9478, 1996.

441 Pazmiño, A., Godin-Beekmann, S., Hauchecorne, A., Claud, C., Khaykin, S., Goutail, F., Wolfram, E., Salvador,
442 J., Quel, E.: Multiple symptoms of total ozone recovery inside the Antarctic vortex during austral spring, *Atmos.*
443 *Chem. Phys.*, 18, 7557–7572, <https://doi.org/10.5194/acp-18-7557-2018>, 2018.

444 Polvani, L. M., Previdi, M., England, M. R., Chiodo, G., Smith, K. L.: Substantial twentieth-century Arctic
445 warming caused by ozone-depleting substances, *Nat. Clim. Chang.*, 10, 130–133, [https://doi.org/10.1038/s41558-](https://doi.org/10.1038/s41558-019-0677-4)
446 019-0677-4, 2020.

447 Polvani, L. M., Waugh, D. W., Correa, G. J. P., Son, S. -W.: Stratospheric ozone depletion: The main driver of
448 twentieth-century atmospheric circulation changes in the Southern Hemisphere, *J. Clim.*, 24(3), 795–812, 2011.

449 Rowland, F. S., Spencer, J. E., Molina, M. J.: Stratospheric formation and photolysis of chlorine nitrate, *J. Phys.*
450 *Chem.*, 80, 2711-2713, 1976.

451 Roy, R., Kuttippurath, J., Lefèvre, F., et al.: The sudden stratospheric warming and chemical ozone loss in the
452 Antarctic winter 2019: comparison with the winters of 1988 and 2002, *Theor. Appl. Climatol.*, 149, 119–130,
453 <https://doi.org/10.1007/s00704-022-04031-6>, 2022.

454 Salby, M., Titova, E., Deschamps, L.: Rebound of Antarctic ozone, *Geophys. Res. Lett.*, 38, L09702,
455 <https://doi.org/10.1029/2011GL047266>, 2011.

456 Santee, M., MacKenzie, I. A., Manney, G., Chipperfield, M., Bernath, P. F., Walker, K. A., Boone, C. D.,
457 Froidevaux, L., Livesey, N., Waters, J. W.: A study of stratospheric chlorine partitioning based on new satellite
458 measurements and modeling, *J. Geophys. Res.*, 113, D12307, <https://doi.org/10.1029/2007JD009057>, 2008.

459 Shen, X., Wang, L., Osprey, S.: Tropospheric forcing of the 2019 Antarctic sudden stratospheric warming,
460 *Geophys. Res. Lett.*, 47, e2020GL089343, <https://doi.org/10.1029/2020GL089343>, 2020.

461 Shen, X., Wang, L., Osprey, S.: The Southern Hemisphere sudden stratospheric warming of September 2019, *Sci.*
462 *Bull.*, <https://doi.org/10.1016/j.scib.2020.06.028>, 2020.

463 Solomon, S., Ivy, D. J., Kinnison, D., Mills, M. J., Neely, R. R. III, Schmidt, A.: Emergence of healing in the
464 Antarctic ozone layer, *Science*, 252, 269–274, <https://doi.org/10.1126/science.aae006>, 2016.

465 Solomon, S.: Stratospheric ozone depletion: A review of concepts and history, *Rev. Geophys.*, 37, 275–316,
466 <https://doi.org/10.1029/1999RG900008>, 1999.

467 Solomon, S., Haskins, J., Ivy, D. J., Min, F.: Fundamental differences between Arctic and Antarctic ozone
468 depletion, *Proc. Natl. Acad. Sci. U.S.A.*, 111, 6220–6225, <https://doi.org/10.1073/PNAS.1319307111>, 2014.

469 Stolarski, R. S., Cicerone, R. J.: Stratospheric chlorine: A possible sink for ozone, *Can. J. Chem.*, 52, 1610-1615,
470 1974.

- 471 Stone, K. A., Solomon, S., Kinnison, D. E., Mills, M. J.: On Recent Large Antarctic Ozone Holes and Ozone
472 Recovery Metrics, *Geophys. Res. Lett.*, 48, e2021GL095232, <https://doi.org/10.1029/2021GL095232>, 2021.
- 473 Strahan, S. E., Douglass, A. R.: Decline in Antarctic ozone depletion and lower stratospheric chlorine determined
474 from Aura Microwave Limb Sounder observations, *Geophys. Res. Lett.*, 45, 382–390,
475 <https://doi.org/10.1002/2017GL074830>, 2018.
- 476 Tully, M. B., Klekociuk, A. R., Krummel, P. B., Gies, H. P., Alexander, S. P., Fraser, P. J., Henderson, S. I.,
477 Schofield, R., Shanklin, J. D., Stone, K. A.: The Antarctic ozone hole during 2015 and 2016, *J. South.
478 Hemisphere Earth Syst. Sci.*, 69, 16, <https://doi.org/10.1071/ES19021>, 2019.
- 479 Vargin, P. N., Nikiforova, M. P., Zvyagintsev, A. M.: Variability of the Antarctic Ozone Anomaly in 2011–2018,
480 *Russ. Meteorol. Hydrol.*, 45, 63–73, <https://doi.org/10.3103/S1068373920020016>, 2020.
- 481 Wargan, K., Weir, B., Manney, G. L., Cohn, S. E., Livesey, N. J.: The anomalous 2019 Antarctic ozone hole in
482 the GEOS constituent data assimilation system with MLS observations, *J. Geophys. Res.*, 125, e2020JD033335,
483 <https://doi.org/10.1029/2020JD033335>, 2020.
- 484 Weatherhead, E. C., Reinsel, G. C., Tiao, G. C., Jackman, C. H., Bishop, L., Hollandsworth Frith, S. M., DeLuisi,
485 J., Keller, T., Oltmans, S. J., Fleming, E. L., Wuebbles, D. J., Kerr, J. B., Miller, A. J., Herman, J., McPeters, R.,
486 Nagatani, R. M., Frederick, J. E.: Detecting the recovery of total column ozone, *J. Geophys. Res.-Atmos.*, 105,
487 22201–22210, <https://doi.org/10.1029/2000JD900063>, 2000.
- 488 Wespes, C., Hurtmans, D., Chabrillat, S., Ronsmans, G., Clerbaux, C., Coheur, P.-F.: Is the recovery of
489 stratospheric O₃ speeding up in the Southern Hemisphere? An evaluation from the first IASI decadal record
490 (2008–2017), *Atmos. Chem. Phys.*, 19, 14031–14056, <https://doi.org/10.5194/acp-19-14031-2019>, 2019.
- 491 Williamson, D. L., Rasch, P. J.: Two-dimensional semi-Lagrangian transport with shape-preserving interpolation,
492 *Mon. Weather Rev.*, 117, 102–129, 1989.
- 493 WMO (World Meteorological Organization): Scientific Assessment of Ozone Depletion: 2006, Global Ozone
494 Research and Monitoring Project – Report No. 50, 572 pp., Geneva, 2007.
- 495 WMO (World Meteorological Organization): Scientific Assessment of Ozone Depletion: 2014, Global Ozone
496 Research and Monitoring Project Report, World Meteorological Organization, Geneva, Switzerland, 416 pp.,
497 2014.
- 498 World Meteorological Organization (WMO): WMO Antarctic Ozone Bulletins (2015), [Available online at
499 www.wmo.int/pages/prog/arep/WMOAntarcticOzoneBulletins2015.html], 2015.

500 Yamazaki, Y., Matthias, V., Miyoshi, Y., Stolle, C., Siddiqui, T., Kervalishvili, G., et al.: September 2019
501 Antarctic sudden stratospheric warming: Quasi-6-day wave burst and ionospheric effects, *Geophys. Res. Lett.*,
502 47, e2019GL086577, <https://doi.org/10.1029/2019GL086577>, 2020.

503 Yang, E.-S., Cunnold, D. M., Newchurch, M. J., Salawitch, R. J., McCormick, M. P., Russell, J. M., Zawodny, J.
504 M., Oltmans, S. J.: First stage of Antarctic ozone recovery, *J. Geophys. Res.*, 113, D20308,
505 <https://doi.org/10.1029/2007JD009675>, 2008.

506 Zuev, V., Savelieva, E.: The cause of the strengthening of the Antarctic polar vortex during October–November
507 periods, *J. Atmos. Solar-Terrestrial Phys.*, 190, <https://doi.org/10.1016/j.jastp.2019.04.016>, 2019.

508
509
510
511
512

513